G3: Genes|Genomes|Genetics Early Online, published on August 15, 2016 as doi:10.1534/g3.116.031229

A *Drosophila* LexA Enhancer-Trap resource for developmental biology and neuroendocrine research

Lutz Kockel[1], Lutfi M. Huq[2*], Anika Ayyar[2*], Emma Herold[2*], Elle MacAlpine[2*], Madeline Logan[2*], Christina Savvides[2*], Grace E.S. Kim[3*], Jiapei Chen[2*], Theresa Clark[2*], Trang Duong[2*], Vahid Fazel-Rezai[2*], Deanna Havey[2*], Samuel Han[2*], Ravi Jagadeesan[2*], Eun Soo Jackie Kim[2*], Diane Lee[2*], Kaelina Lombardo[2*], Ida Piyale[2*], Hansen Shi[2*], Lydia Stahr[2*], Dana Tung[2*], Uriel Tayvah[2*], Flora Wang[2*], Ja-Hon Wang[2*], Sarah Xiao[2*], Sydni M. Topper[4], Sangbin Park[1], Cheryl Rotondo[5], Anne E. Rankin[5], Townley W. Chisholm[5] and Seung K. Kim[1,6,7]

[1]Dept. of Developmental Biology, Stanford University School of Medicine, Stanford CA 94305

[2]Phillips Exeter Academy, Exeter, NH 03833

[3]Palo Alto High School, Palo Alto, CA 94306

[4]Pinewood School, Los Altos, CA 94022

[5]Science Department, Phillips Exeter Academy, Exeter, NH 03833

[6]Dept. of Medicine (Oncology Division) Stanford University School of Medicine, Stanford CA 94305

*These authors contributed equally

[7]Corresponding author

Abstract

Novel binary gene expression tools like the LexA-LexAop system could powerfully enhance studies of metabolism, development and neurobiology in *Drosophila*. However, specific LexA drivers for neuroendocrine cells and many other developmentally relevant systems remain limited. In a unique high school biology course, we generated a LexA-based enhancer trap collection by transposon mobilization. The initial collection provides a source of novel LexA-based elements that permit targeted gene expression in the corpora cardiaca, cells central for metabolic homeostasis, and other neuroendocrine cell types. The collection further contains specific LexA drivers for stem cells and other enteric cells in the gut, and other developmentally relevant tissues types. We provide detailed analysis of nearly 100 new LexA lines, including molecular mapping of insertions, description of enhancer-driven reporter expression in larval tissues and adult neuroendocrine cells, comparison with established enhancer trap collections and tissue specific RNAseq. Generation of this open-resource LexA collection facilitates neuroendocrine and developmental biology investigations, and shows how empowering secondary school science can achieve research and educational goals.

Introduction

Differential gene expression in specific cells, at specific times and levels, is a principal driver of animal development and physiology. Research in *Drosophila melanogaster* has been invaluable for understanding the genetic basis of development and physiology. Based on strategies from bacterial genetics (Kroos and Kaiser, 1984), investigators have developed transposon-based methods to detect enhancer activity ('enhancer trapping') following random insertion mutagenesis (O'Kane and Gehring, 1987). The activity of *Drosophila* enhancer elements was first detected by the expression of randomly inserted P-elements carrying a weak promoter fused to a *lacZ* reporter gene (O'Kane and Gehring, 1987).

To investigate and manipulate *Drosophila* gene expression in time and space, investigators have also exploited the activity of endogenous *cis*-regulatory enhancer elements to control expression of transactivators or repressors in specific temporal or spatial patterns of larval and adult tissues. Deployment of the yeast Gal4 transactivator to 'drive' expression of target genes fused to GAL4-responsive upstream activating sequences (UAS), established a binary gene expression system in *Drosophila* (Brand and Perrimon 1993; Hayashi et al., 2002; Gohl et al., 2011).

However, novel challenges in studying biological problems like inter-cellular or inter-organ communication necessitate parallel manipulation of two or more independent cell populations (Rajan and Perrimon 2011). This requires additional binary expression systems independent of UAS-Gal4, such as the bacterial derived LexA system, which is based on LexA DNA binding domain:transactivator domain fusion proteins that regulate expression of transgenes fused to a LexA operator-promoter (LexAop; Szuts and Bienz 2000; Lai and Lee 2006; Pfeiffer et al., 2010; Knapp et al., 2015, Gnerer et al. 2015). The simultaneous use of two binary expression systems permits

powerful epistasis experiments between different tissues (Shim et al., 2013), simultaneous clonal analysis of multiple cell populations (Lai and Lee 2006, Bosch 2015), and visualization of specific physical cell-cell contacts (Gordon and Scott 2009; Bosch et al., 2015, Macpherson et al. 2015). However, successful use of combinations of binary expression systems largely depends on the availability of transgenic driver lines for specific developmental biology and physiology approaches. Within the framework of a high school science class developed in partnership between groups at Stanford University and Phillips Exeter Academy we constructed the StanEx collection of LexA-based enhancer trap drivers for neuroendocrine and developmental biology research.

Methods:

Generation of StanEx1 P-element: The StanEx enhancer trap P-element carries the weak P-promoter linked to a fusion of the LexA DNA binding domain-Gal4 hinge- Gal4 transcriptional transactivation domain (Pprom-LHG). To make pJFRC-MUH-70LHG70, 3563bp Eag1-Eag1 fragment from pDPPattB-LHG (Yagi et al., 2010) was subcloned to 7097bp Eag1-Eag1 fragment from pJFRC-MUH (Pfeiffer et al., 2010). To make pBS2KSP-attP-Pprom-GAL4-hsp70 3'UTR, 3615bp Not1-Not1 fragment from pXN-attPGAL4LWL (Gohl et al., 2011) was subcloned to Not1 site on pBS2KSP vector. To make pBS2KSP-attP-Pprom-LHG-hsp70 3'UTR, 3563bp (Eag1)-(Eag1) fragment from pJFRC-MUH-70LHG70 was Klenow filled-in, and ligated to 3259bp (BamH1)-(BamH1) fragment from pBS2KSP-attP-Pprom-GAL4-hsp70 3'UTR that was Klenow filled-in. 3941bp Sac2-Xba1 fragment from pBS2KSP-attP-Pprom-LHG-hsp70 3'UTR (Xba1 in LHG coding region is methylated) was subcloned to 8453bp Sac2-Xba1 fragment from pXN-attPGAL4LwL (Gohl et al., 2011). P-element vector into y[1],w[1118] strain transformation was performed by standard procedures to generate the StanEx[SP001] X-liked index insertion.

Immuno-histochemistry (IHC): All tissues were fixed in 4% Formaldehyde/PBS for 30 min, permeabilized in 0.2% Triton X-100/PBS for 4 hours and blocked in 3% BSA/PBS for 1 hour. All antibody stainings were performed in 3% BSA/PBS, incubation of primary and secondary antibodies were O/N. PBS was used for all rinses and washes (3x each for primary and secondary antibody incubation steps). Antibodies used: Chicken anti-RFP 1:2000 (Rockland, 600-901-379). Goat anti-GFP 1:3000 (Rockland 600-101-215). Mouse anti-Tubulin 1:5000 (Sigma T5168). Donkey anti-Goat Alexa488 (Life Technologies, A11055). Donkey anti-Chicken Cy3 (Jackson ImmunoResearch 703-165-155). Donkey anti-Mouse Alexa594 (Life Technologies A21203). All

secondary antibodies were used at 1:500. All samples were mounted in SlowFade Gold mounting medium with DAPI (Life Technologies, S36938).

Microscopy: Microscopy was performed on a Zeiss AxioImager with filter sets 49, 38HE, 43HE and 64HE for DAPI, Alexa488, Cy3 and Alexa 594, respectively, using the extended focus function. Confocal microscopy was performed using a Leica TCS SP5 using a Ti-Saphire multiphoton laser for DAPI, and the 488nm Argon, 546nm and 594nm HeNe laser lines and HyD GaAsP detectors.

Fly husbandry and fly strains: All fly strains were maintained on a standard cornmeal-molasses diet (http://flystocks.bio.indiana.edu/Fly_Work/media-recipes/molassesfood.htm). The following strains were used: y[1],w[1118] (Bloomington 6598), w[*]; ry[506] Sb[1] P{ry[+t7.2]= Δ2-3}99B/TM6B, Tb[1] (Bloomington 1798), w[*]; P{y[+t7.7] w[+mC]=26XLexAop2-mCD8::GFP}attP2 (Bloomington 32207), w[*]; L[*]/CyO; ftz[*] e[*]/TM6,Tb[*]; *StanEx*^{1} is the X-liked index insertion of the StanEx enhancer trap P-element collection utilizing the P-element promoter – LexA DNA binding domain "L"– Gal4 hinge region "H" – Gal4 transcriptional activation domain "G" construct (see above), y[1],w[1118]; P{w[mC]=LHG]StanEx[1]}. We noted LexA-independent detection of 26x*LexAop2-CD8::GFP* in garland and pericardial nephrocytes at the L3 stage (Suppl. Figure 6).

Hybrid dysgenesis: Males of donor stock y,w,StanEx[1] were mated to w[*]; ry[506],Sb[1],Δ2-3/TM6B,Tb[1], and 10 F_1 "jumpstarter" y,w,StanEx[1]; ry[506],Sb[1], Δ2-3/+ males were crossed to 20 double-balancer virgin females. *w*+ F_2 males were mated to w[*];

L[*]/CyO; ftz[*] e[*]/TM6,Tb[*], the autosome of insertion was determined, and the insertion line stably balanced (Ryder et al., 2004). In the first iteration of the Bio470 class (see below), multiple *w+* F_2 males originating from the identical male jumpstarter parent were isolated into a stock leading to an artificially high rate of identical insertions. This practice was discontinued. One line with an X-chromosome insertion was isolated (*StanEx*$^{AA10.1}$), despite our intercross scheme for exclusively isolating autosomally-linked insertions (Supplementary Table 1).

Insertion site cloning: We followed an inverse PCR approach (Ochman et al., 1988, http://www.fruitfly.org/about/methods/inverse.pcr.html), to molecularly clone the insertion sites of StanEx P-elements. Overall, we sequenced genomic DNA adjacent to both 5' and 3' P-element sequences in 91% of the lines, and identified unique genomic sequence adjacent to at least one end of the P-element in the remaining lines. DNA restriction enzymes used: BfuCI (NEB R0636), HpaII, (NEB R0171). Ligase used: T4 DNA Ligase (NEB M0202). Inverse PCR primer "Plac1" CAC CCA AGG CTC TGC TCC CAC AAT and "Plac4" ACT GTG CGT TAG GTC CTG TTC ATT GTT were used to clone genomic sequences off the 5' end of P-element. Inverse PCR primer "Kurt" TGT CCG TGG GGT TTG AAT TAA C and "Ulf" AAT ACT ATT CCT TTC ACT CGC ACT were used to clone genomic sequences off the 3' end of P-element. Sequencing primer "Sp1" ACA CAA CCT TTC CTC TCA ACA A was used for 5' end of P-element. Sequencing primer "Berta" AAG TGG ATG TCT CTT GCC GA was used for 3' end of P-element. For insertions where the sequence of one end only could be determined by inverse PCR, we pursued a gene-specific PCR approach (Ballinger and Benzer 1989) using P-element and gene-specific primers. 5' end specific P-element primer "Chris": GCA CAC AAC CTT TCC TCT CAA C. 3' end specific P-element primer "Dove": CCA CGG ACA TGC TAA GGG TTA A. Line specific primers sequences: LH4-5: CTTTGAGTACGCCCCACATTTG; RJ4-3:

GCAAAATCTGATGACCCTGCTG; EM9-3: TGCCCAATCACTTGTGTCAAAA; DL5-3: TGTGTGAGTGTGCGAGTAAAGA; CS2-3ONE: ATGCAACACGTATTGGCACTTC; CS2-5: GAACAAGGTCAAGTGTCATCGC; CS2-3TWO: ATGAGCGCTTGAGATTCGGTAT; DRH4-3: TTGGGAAAGTCTACGGTGAGTG; IP1-3: GGAGCGAGATAAATACGAGGGG; IP3-3: AGTGGCGGGTTGAAACTAGAAT; SJH2-3: TGGGGAGTGTGAAATGTGCATA; AT5-3: TAGCTGACACCTGTTACCTTGG; AA14-5: AATTGCAATCGAATCGGGTTGG; AT1-5: CAGCTCGTTACGCAGGATTTTG; EH7-5: GCATTAGGTGGAGCTGCATTTC; EM7-3: GCCGAACGAGCAATTATACCAC; EM14-3: TTCTCTCCCAACCCAAACCAAA; EM15-3: GGAAAACTTCTCGCTGCAGTTT; EM16-3: AAGAAAGGAGGATGGCAAGGAG; JHW2-3: GACTCATTTGTTTCTGGTGGCC; JPC2-3: ACAATGCTGCAACACTTCTTCC; UT5-3: GTTGTAGTTGGTGGCGCATATC; TC1-5: AAGTATCCAAGCCAAGAAACCAC; TD1-3: CGGTTCGTTTACAATACGGCAG; TD1-5: ACCTTATCAGAGCAGGAGAAAACC

A subset of inverse and direct PCRs were performed by LakePharma, Belmont, CA. Sequencing was performed by Sequetech Corp, Mountain View, CA.

Clustering of tissue-specific patterns

Imaging data was digitized by tissue specific expression (0=no expression, 1=expression), and hierarchical clustering using Euclidian distance and complete linkage was performed using Cluster 3.0 software, and visualized deploying TreeView.

Nomenclature of P-element insertion site: Independently of the direction of insertion, we defined the first nucleotide 3’ of the actual insertion into the genomic scaffold as insertion site of the individual StanEx P-elements.

Coursework at Phillips Exeter Academy and Stanford University: In the 11-week spring term for 2013 and 2014, 12 students were selected for an elective advanced class called Bio470, with a pre-requisite/co-requisite of advanced placement (AP) biology or one term of a genetics elective. Bio470 was comprised of 4 scheduled 50 minute periods and a 70-minute period, and approximately 5-6 unscheduled hrs per week. This format transformed a standard biology classroom into an open laboratory. The course manual, weekly schedule and problem sets are available on request. Problem sets, reading and discussions covered transmission genetics using balancer chromosomes, the biology of mobile genetic elements, and methods including inverse PCR, molecular cloning and antibody-based staining techniques. After learning basic *Drosophila* genetic methods, students spent approximately 8-9 weeks executing the hybrid dysgenesis crosses detailed in Supplementary Figure 2. Mapping and balancer intercrosses ensued, in parallel with initial molecular mapping studies with polymerase-chain reaction and DNA sequencing using standard genomic DNA recovery (see above). Intercrosses with *LexAop2-CD8::GFP* reporter strains were initiated in the last 3 weeks, permitting instruction in larval dissection and microscopy to document tissue expression patterns of candidate enhancer traps. Refurbished Zeiss Axiophot microscopes were provided by S.K.K. and the department of Developmental Biology (Stanford) to Bio470. Based on performance in Bio470, two to three Exeter students, and high school students from Palo Alto, CA or Los Altos, CA, were selected to continue studies in the Kim group at Stanford University School of Medicine during summer internships lasting about 6 weeks. These studies included further molecular mapping of transposon insertion sites, and verification of tissue patterns of enhancer trap expression. Students returning in the fall term helped instructors to run the subsequent iteration of Bio470, and also pursued independent projects.

Data and reagent availability: StanEx fly strains will be submitted to the Bloomington stock center. The course manual, weekly schedule and problem sets are available on request. Figure S1 shows a schematic of the StanEx P-element. Figure S2 describes the hybrid dysgenesis crossing scheme. Figure S3 displays the clustering of tissue specific expression data across StanEx lines. Figure S4 presents immuno-histochemical analysis of StanEx enhancer traps in larval proventriculus. Table S1 contains the molecular and expression data of the StanEx enhancer trap collection. Table S2 summarizes StanEx enhancer trap lines analyzed for expression in adult flies.

Results

Generating a LexA-based enhancer trap collection

To build a LexA-based enhancer trap collection, we modified the InSITE P-element vector (Gohl et al., 2011; Supplementary Figure 1). A cDNA encoding the LexA DNA-binding domain fused to the hinge-transactivation domain of Gal4 (LexA::HG, Yagi et al., 2010) was inserted between the attP and loxP sites of the P-element vector (Supplementary Figure 1, see Methods). This configuration sensitizes the P-element promoter expression to local genomic enhancer activity. This P-element vector also enables subsequent recombinase-mediated cassette exchange (RMCE; Gohl et al. 2011). We transformed an index X-chromosomal-linked fly strain, named *StanEx*^{1} (Supplementary Table 1: see Methods). Progeny from intercross of *StanEx*^{1} with a line harboring a LexA operator- GFP reporter transgene (*LexAop2-CD8::GFP*; Pfeiffer et al., 2010) had clear membrane-associated GFP expression in several tissues including ring gland, imaginal discs of the wing, eye, haltere and T3 leg, eye imaginal disc, midgut and fat body (Figure 1 and Supplementary Figure 5), confirming suitability of *StanEx*^{l} as a starter line for transposase-mediated hybrid digenesis. We then mobilized the *StanEx*^{1} P-element insertion to autosomes using standard hybrid dysgenesis methods, to generate LexA P-element insertion lines (Supplementary Figure 2; Methods; O'Kane, 1987; Pfeiffer et al., 2008). Using *StanEx*^{1} P-element mobilization we obtained 149 initial lines.

Mapping *LexA* P-element insertion sites

Standard molecular methods were used to map the chromosomal insertion position (Figure 2, Supplementary Table 1; http://stanex.stanford.edu/about/). After eliminating lines with identical

insertions (see Methods), we identified 93 lines with a unique insertion position (Supplementary Table 1). The insertions were distributed across the autosomes, with each arm of chromosomes 2 and 3 receiving approximately a quarter of the insertions (2L: 23 insertions, 2R: 23 insertions, 3L: 20 insertions, 3R: 24 insertions). Three insertions were linked to repetitive sequences, precluding mapping of the chromosomal integration site (*StanEx*^{DT3}, *StanEx*^{AA2}, *StanEx*^{FW4}).

The majority of insertions were linked to specific genes, including many developmental regulators. Three independent insertions (*StanEx*^{SX4}, *StanEx*^{SJH1} and *StanEx*^{RJ4}; Supplementary Table 1) were located in the region 5' of the transcriptional start site of *escargot* (esg), a known 'hot-spot' for P-element insertion (Bellen et al., 2004, Hayashi et al., 2002). Two insertions mapped within 4.5kb at the locus encoding *Meltrin* (*StanEx*^{JPC10} and *StanEx*^{DRH2}), and two insertions mapped within the first intron of *CG31145* (*StanEx*^{JPC7} and *StanEx*^{EM7}). We also recovered two insertions in *NK7.1*, which showed reverse orientation (*StanEx*^{RJ3} and *StanEx*^{EH4}). Overall, mapping of the 93 StanEx P-element insertions revealed a strong bias for insertion in the 5' end of genes: 72% of all insertions were mapped to within 300 bp of the 5' regulatory sequence preceding the transcriptional unit (41%) or its first exon (32%). In one line, the P-element inserted in the region distal to the 3' end of the nearest gene (*StanEx*$^{SX-5}$, inserted near *CR43276*). 69% of the StanEx insertions mapped to loci previously shown to harbor 5 or more P-elements insertions within +/– 100 bp (Bellen et al., 2011). To our knowledge, LexA lines or other LexA-based tools have not been previously described for these 64 loci. Further, we isolated an additional 17 lines in which *StanEx*^{1} inserted in unique sites with no known P-element insertions within this radius. Some of these unique insertions include developmentally important genes, such as *NK7.1*, *ptip, Tom7, mir-992/Nnf1a, CG7149, CadN, CG31145, Meltrin, nemo, CG3092/yip3, rdx, W* and *bsg (intergenic).* Thus, our approach generated multiple novel LexA-based autosomal enhancer traps.

Tissue expression of *LexA* in the StanEx collection

To evaluate the tissue expression patterns of the insertion lines, we intercrossed the *LexA::HG4* transcriptional activator insertion lines to flies harboring a *LexAop2-CD8::GFP* reporter (Pfeiffer et al., 2010). 3rd instar larvae of bi-transgenic offspring were analyzed by immuno-histochemical (IHC) staining for GFP expression using a counterstain for microtubules (anti-tubulin) and cell nuclei (DAPI). Image data from 91 LexA lines were collected and organized into a searchable public database (see below). Within the collection, we detected expression in nearly all tissues of the L3 larva, including a variety of neuronal cell types in the CNS, VNC (Figure 3) and PNS, imaginal discs, and a wide range of other somatic tissues like fat body, malpighian tubules and trachea (Figure 4). We also observe LexA expression in a subset of cells in the midgut with features of gut stem cells (Figure 4C, $StanEx^{SX4}$, inserted in escargot, Korzelius et al., 2014), and entero-endocrine cells ($StanEx^{LH4}$, Figure 4F, inserted in *numb-associated kinase*, Takashima et al., 2011).

To facilitate further comparison of the StanEx collection lines to other expression data sets, we analyzed a subset of 76 StanEx lines that are unambiguously inserted within or adjacent to a single known gene. On average, each StanEx line expressed LexA activity in 5 distinct cell types (Suppl. Figure 3). One line expressed in a single tissue only ($StanEx^{FW3}$). These findings are consistent with prior studies indicating that enhancers only very rarely produce expression patterns limited to a single cell type in a complex organism (Jenett et al., 2012). In 3 lines we did not detect any discernible GFP expression, indicating the absence of inherent LexA expression from these StanEx P-element insertions ($StanEx^{DL-3}$, $StanEx^{DRH1}$ and $StanEx^{VF1}$). We reproducibly detected LexA expression in neuronal cells of the CNS in 84% of lines (64/76) and in the VNC of 83% (63/76:

Supplementary Table 1). This includes median protocerebral insulin-producing cells (IPCs; Figure 3C, arrowheads Figure 3C'), a group of cells neighboring IPCs, CNS commissural neurons, CNS neurons in the optic lobes and CC cells (arrowheads Figure 3A' and D'). Many lines expressed unique, cell-specific expression patterns. For example, in four StanEx insertion lines we observed reporter expression in a subset of CC (Corpora Cardiaca) cells, a pattern of mosaic expression not previously described to our knowledge (Figure 5, Park et al., 2011). Seven out of 95 StanEx lines drove reporter gene expression in the proventriculus, a larval foregut structure (Supplementary Figure 4). We observed LexA-dependent labeling of distinct proventricular cell subsets in each of these StanEx lines, including subsets of anterior, medial and posterior 'stripes' in the outer visceral mesoderm, the inner epithelial layer, and the cardiac valve. Patterned gene expression in the proventriculus has been described (Singh et al. 2011, Josten and Hoch 2004, Senger et al., 2004) and the novel binary expression resource created here could be useful for studying mechanisms underlying patterning of the proventriculus.

To assess commonalities of expression patterns in the StanEx collection, we performed clustering analysis of the digitized tissue expression pattern of all StanEx lines (Supplementary Figure 3, see Methods). This revealed co-variation between the identified tissue expression domains. For example, with one exception (*StanEx*$^{KDL-1}$, insertion in *bacchus*), all lines expressing in the VNC showed expression in the CNS. Conversely, all CNS expressing lines except two (*StanEx*$^{DRH-2}$, insertion in *meltrin*, *StanEx*$^{SX-10}$, insertion in *hairy*) had detectable expression in the VNC. These findings support the prior suggestion of a 'linked' enhancer code shared by these two tissues (Li et al., 2014).

To facilitate storage of imaging and molecular data, including image archiving, annotation, retrieval, and database mining, we generated the StanEx website (http://stanex.stanford.edu/about/; L. Huq, L. Kockel, S.K., unpubl. data), an online database searchable by expression pattern, cytology and specific genes. This includes supplementary image analysis, data from immunostaining and molecular features of StanEx insertion loci, and is freely accessible for the scientific community. Although database mining is beyond the scope of this report, we present examples below that illustrate the types of studies our data permit.

Comparison of StanEx enhancer trap tissue expression patterns with prior data sets

To verify the quality of our image and histological analysis, we compared analysis from prior data sets reporting tissue-specific RNA expression to reporter-gene expression patterns generated with the StanEx lexA enhancer trap collection. Specifically, we used stage-specific and organ-specific RNA-seq data recently obtained from brain, imaginal discs, digestive system, fat body and salivary gland (Graveley et al., 2011) to query a subset of 71 StanEx lines inserted within a specific gene. Overall, 98 % StanEx lines partially or fully reproduced tissue-specific expression detected previously by RNA-Seq. We also compared the tissue expression pattern of our collection with that from a previously-described Gal4 enhancer trap collection (NP) of the *Drosophila* Genome Resource Center (DGRC; Hayashi et al., 2002). The reported expression pattern of 73% of these NP enhancer traps fully or partially matched the gene expression pattern reported in the RNAseq dataset (Graveley et al., 2011). We found that 52 genes with 274 Gal4-based insertions in the NP collection are also represented in the LexA-based StanEx collection. Direct comparison of the reported expression patterns of NP and StanEx insertions revealed a 91% full or partial overlap.

Thus, our analyses indicate good concordance between StanEx enhancer trap expression and tissue patterns of gene expression derived from RNA-Seq or enhancer trap collections data sets.

Neuroendocrine cell enhancer traps in the StanEx collection

To identify additional uses of the StanEx collection, we focused on drivers for neuroendocrine cells. For example, the insulin producing cells (IPCs) are neuroendocrine cells that produce and secrete the hormone insulin to regulate carbohydrate homeostasis and growth. Complementary to this, corpora cardiaca (CC) cells secrete the polypeptide hormones Akh and Lst, to mobilize energy reserves and regulate insulin secretion (Kim et. al, 2004, Alfa et al. 2015). Experimental dissection of the neuroendocrine cellular circuitry orchestrating hormonal regulation of metabolism should greatly benefit from independent binary LexA-LexAop and GAL4-UAS genetic systems. We identified 47 StanEx enhancer traps that drove reporter gene expression in the ring gland of third instar larvae. Of these 47 lines, 37 drove reporter-gene expression in the CC cells. In addition, insulin producing cells (IPCs) in the pars intercerebralis of the *Drosophila* brain are marked by 13 lines (Supplementary Table 1). A previous study (Harvie et al., 1998) that analyzed the ring gland expression of 510 PZ enhancer traps found 76 lines (15%) showing ring gland expression. An analysis of a subset of these 76 lines revealed 3 lines with CC cell expression. However, the small sample size of molecularly characterized PZ lines (12/76, 16%) precluded comparison between tagged genes in the two collections.

CC cells undergo extensive remodeling during metamorphosis but persist in adults, with connections to the foregut and heart (Alfa et al., 2014; Cognini et al., 2011), while other cells in the larval ring gland comprising the prothoracic gland or corpus allatum degenerate. To determine if

neuroendocrine LexA expression persists after metamorphosis, we analyzed LexA enhancer trap expression produced by adult CC cells in a subset of StanEx lines. We used a dual labeling strategy, marking adult CC cells with akh-G4, UAS-CD4:tandemTomato (Park et al., 2011; Han et al., 2011), and tested if LexA::HG directed expression of the reporter *LexAop2-CD8::GFP* (Pfeiffer et al., 2010). In seven of thirteen (54%) StanEx lines that expressed LexA in larval CC cells, we observed maintenance of LexA expression in adult CC cells. By comparison, 28% of the so-called FlyLight enhancer constructs expressed in larval neurons continued to be expressed in adult neurons (Li et al., 2014). Using a similar strategy for IPCs, we found that 1 of 7 StanEx lines (*StanEx*$^{DL\text{-}5.1}$, insertion in Diap1) maintained LexA::HG expression in adult IPC cells, consistent with prior studies of larval and adult IPCs (Jennett et al., 2014). In three StanEx lines, we reproducibly observed labeling of IPC and CC cell subsets (*StanEx*$^{EH\text{-}4}$, insertion in *NK7.1*, *StanEx*$^{UT\text{-}4}$, insertion in *Rho1*, *StanEx*$^{DT\text{-}1}$, insertion close to *CR43857*, Figure 5). Thus, our findings provide evidence for heterogeneous gene expression in individual IPCs and CC cells, supporting the view that these cells may have diversified function (Kim et al., 2015; Rajan and Perrimon, 2012). The ability to discriminate individual cells within a cluster should prove useful for studies of dynamic synapse development or remodeling, a possibility previously raised in other neurotransmitter or hormone-producing cell types (De Paola et al., 2006).

Discussion

Here we used transposase-mediated P-element mobilization to trap enhancers that express a chimeric LexA::HG4 fusion. We generated a collection of *Drosophila* lines that should prove useful for genetic, developmental and physiological studies of cells and tissues. The ability to use LexA::HG4 in combination with other binary systems like UAS-GAL4 should advance studies of short-range and long-range cell interactions and inter-organ signaling in vivo, a growing area of investigation in *Drosophila.* The resources described here should prove valuable for a range of investigations, in particular for neuroendocrine research, and were generated from two consecutive iterations of a high school biology course. This illustrates the feasibility of building partnerships between research universities and secondary schools to conduct biological research with practical outcomes.

P-element insertion in flies is non-random (O'Hare and Rubin, 1983; Berg and Spradling, 1991), with a strong bias for transposition to the 5' end of genes (Spradling et al., 1995). P-element insertion preferences are likely guided by the chromatin state and other structural features of the target DNA rather than a sequence-based DNA motif (Liao et al., 2000). We find a similar preference in the StanEx P-element, with approximately 72% of the insertions in the promoter or 5' UTR regions of genes. Similar to outcomes from studies of KG element mobilization (Bellen et al., 2004), we note that the sites of multiple P element insertions (hotspots) in our study were within one cytological unit of breakpoints in the CyO and TM6B chromosomes, balancer chromosomes used in our hybrid dysgenesis protocol, indicating points of greater chromosome accessibility.

The LexA::HG StanEx enhancer traps display a significant degree of overlapping expression patterns when compared to Gal4 enhancer traps inserted near the same site, and also overlap

significantly with existing RNAseq data (Hayashi et al., 2002; Graveley et al., 2011). Hence, the weak P-element promoter linked to the LexA::HG reporter of the StanEx1 P-element represents a reliable enhancer trap. Multiple StanEx lines revealed distinct expression patterns in many developmentally and physiologically key cell populations and tissues. For example, we isolated several LexA enhancer traps driving expression in neuroendocrine cells like IPCs and CC cells, including enhancer traps reproducibly expressed in subsets of IPCs or CC cells. Based on the expression of secreted neuropeptides, previous reports have indicated a subdivision within the IPC neuroendocrine cell clusters (Kim and Neufeld 2015). However, genetic elements permitting targeting of IPC or CC cell subsets have not been previously available, to our knowledge. The new genetic tools described here should enable the further analysis of the IPC-CC inter-relationships and foster characterization of possible cell diversification within these neuroendocrine clusters. Several StanEx lines also show unique expression patterns in the proventriculus of the third instar larva. The proventriculus is an organ derived from at least three tissue layers, visceral mesoderm, ectodermal epithelial layer and the cardiac valve (Pankratz and Hoch, 2002). We observed reporter expression restricted in antero-posterior stripes, in both inner and outer cell layers of the proventriculus. Restricted expression patterns in the proventriculus have been noted for genes encoding GATA factors (Senger et al., 2006), the dve transcription factors (Kölzer et al., 2003) and STAT92E (Singh el al., 2011). To our knowledge, few layer- and pattern-specific genetic tools have been reported for this organ, and none based on LexA.

We observed a high degree of partial or full overlap between the enhancer trap activity displayed by the individual StanEx insertion lines and the respective counterparts of the NP Gal4 enhancer traps (Hayashi et al, 2002), and the reported mRNA expression pattern of the gene the StanEx lines are inserted in (Graveley et al., 2011). We suspect that differences of reported

expression patterns might be due to inherent technical limitations of a bigenic expression system, including delayed production of the GFP reporter protein or variable sensitivity of the minimal P-element promoter in the StanEx enhancer trap element to endogenous enhancers. The regional differences of P-element insertion between the NP Gal4 lines and StanEx enhancer traps within the same gene might represent another factor to account for the observed differences of expression.

The LexA-LexAop binary expression system in the StanEx enhancer trap collection provides opportunities for a variety of intersectional methods with the UAS-Gal4 expression system (Shim et al., 2013; Lai and Lee, 2006; Gordon et al., 2009; Bosch et al., 2015). One advantage for combining these methods is the lack of interfering cross-talk between the LexA-LexAop and Gal4-UAS system. The transcriptional cross-activation of Gal4 to LexAop promoters and of the LexA transcriptional activator on UAS regulatory sequences is minimal, consistent with the independent binding-site specificity of the two systems (Lei and Lee, 2006). With the advent of φC31-attP mediated transformation (Groth et al., 2004), large collections of promoter fragment-driven Gal4 transgenes have been generated at specific attP sites (Jenett et al., 2012). However, the pairing of somatic chromosomes has been shown to give rise to cross-regulation (transvection) of enhancer/promoter elements between homologous chromosomes (Kassis, 2012; Mellert et al., 2012; Bateman et al., 2012). Combination of sister chromosomes harboring distinct transgenes transformed into the same attP site, e.g. promoter1-Gal4 and promoter2-LexA, might trigger transvection, which can severely confound experimental outcomes. By contrast, the random integration of a LexA-containing StanEx enhancer trap will likely be less prone to transvection when used in combination with Gal4, as long as the integration sites of the two transgenes differ significantly. The StanEx enhancer trap collection should complement ongoing projects to generate LexA driver lines with enhancer fusions with site-specific insertion (Jenett et al., 2012), and

constitutes a valuable experimental tool resource. The creation of a searchable on-line StanEx database will enable the scientific community to select the strain of choice, and the associated fly strains (including stocks generated in future iterations of the course) will be available in the public fly stock repositories.

The results, resources and experience detailed here stem from consecutive iterations (2013-2014) of a high school biology course now in its fifth year of enrollment. Fruit fly genetics and developmental biology served as an ideal vehicle for building an authentic, open-ended research program for new scientists, based on key attributes (see Methods) including (1) relative technical simplicity of fly husbandry, (2) conceptual simplicity requiring only modest prior mastery of biology and genetics, transitioning to complex operations like tissue dissection, histology, microscopy, and code-writing to create the StanEx database (3) compatibility with flexible scheduling, (4) concrete achievement milestones for both instructors and students, (5) project ownership, (6) publishable results and (7) cost feasibility in the setting of a modern genetics curriculum (Redfield, 2012). Our experimental strategies had the advantage of offering each student a reasonable prospect of isolating one or more novel fly strains, thereby promoting a sense of discovery and ownership (Hatfull et al., 2006), a key research and educational goal. We recognize that the timeframe of the course limited opportunities for experimental design by students. However advantages from this compression included a requirement for a parallel project structure transitioning to longitudinal studies (one class continues work from the preceding class). This continuity enhanced opportunities for students to mentor peers, and to interact with instructors as colleagues. For adult instructors, the course offered unusual opportunities for career development outside a more traditional classroom setting. Fruit fly genetics has been previously used to introduce research to a large consortium of undergraduates (Call et al., 2007). Our experience demonstrates

that longitudinal studies involving multi-generational genetics, animal husbandry, molecular biology, immunohistochemistry and bioinformatics can thrive in a secondary school setting.

Figure Legends

Figure 1: Expression pattern of StanEx^{1} enhancer trap in tissues of wandering third instar larvae visualized by lexAop-CD8:GFP. This fly strain was used as a starter strain for the hybrid dysgenesis. Green: Anti-GFP, Red: Anti-Tubulin, Blue: DAPI. Scale bar = 100 um. For GFP channel only (green) see suppl. Figure 5.

A) CC cells in ring gland .
B) Expression in imaginal disc of wing, leg and haltere.
C) Eye disc.
D) Midgut. Note that expression in garland nephrocytes is lexAop-CD8:GFP background signal (see Methods and Suppl. Figure 6).
E) Fat body.

Figure 2: Distribution of novel StanEx LexA::HG enhancer trap insertions sites in chromosomes I, II and III. See Suppl. Table 1 for corresponding detailed data. Multiple insertions have been obtained in esg, NK7.1, CG31145 and bacc.

Figure 3: Immuno-histochemical analysis of individual StanEx enhancer trap line expression in larval brain and VNC. Third larval instar CNS and VNC expression of LexA::HG is visualized by *LexAop-CD8::GFP*. Green: Anti-GFP, Red: Anti-Tubulin, Blue: DAPI. Scale bar = 100 um.

A-A') *w; StanEx^{DT-2}/ LexAop-CD8::GFP*. Arrowheads in A' mark CC cells.

B-B') *w; StanEx^{EM-16}/ LexAop-CD8::GFP*.

C-C') *w; StanEx^{LH4}/+; LexAop-CD8::GFP/+*. Arrowheads in C' mark IPC cells.

D-D') *w; StanEx^{EJK-1}/LexAop-CD8::GFP*. Arrowheads in D' mark CC cells.

E-E') *w; StanEx^{EH-2}/LexAop-CD8::GFP*.

F-F') *w; StanEx^{EM-7}/LexAop-CD8::GFP*.

Figure 4: Immuno-histochemical analysis of StanEx enhancer trap expression in third instar larval tissue visualized by *LexAop-CD8::GFP*. Green: Anti-GFP, Red: Anti-Tubulin, Blue: DAPI. Scale bar = 50 um.

A) *w; StanEx^{DT-2}/LexAop-CD8::GFP*. Expression in fat body. Note the variable expression in fat body cells.

B) *w; StanEx^{EH-2}/LexAop-CD8::GFP*. Expression in anterior midgut. Note that expression in garland nephrocytes is lexAop-CD8:GFP background signal (see Methods and suppl. Figure 6).

C) *w; StanEx^{SX-4}/+; LexAop-CD8::GFP/+*. Expression in midgut.

D) *w; StanEx^{LH-3}/+; LexAop-CD8::GFP/+*. Expression in malphigian tubules. Note the variable expression in individual cells.

E) *w; StanEx^{HS-2}/LexAop-CD8::GFP*. Expression in trachea located on midgut.

F) *w; StanEx^{LH-4}/LexAop-CD8::GFP*. Expression in small cells in midgut consistent with expression patterns of entero-endocrine cells.

G) *w; StanEx^{JHW-2}/LexAop-CD8::GFP*. Expression in photoreceptor clusters in third instar eye disc.

H) *w; StanEx^{IP-1}/+; LexAop-CD8::GFP/+*. Expression in third instar haltere, leg and wing disc.

Figure 5: Heterogeneous enhancer trap expression in endocrine CC cells and IPCs. Scale bar in A", B" and C" indicates 20 um.

A-A") *w; StanEx^{EH-4} /LexAop-CD8::GFP*. Green: Anti-GFP, Red: Anti-Akh, marking all CC cells, Blue: DAPI. a') Anti-GFP-channel only. a") Anti-Akh channel only

B-B") *w; StanEx^{UT-4}/+; LexAop-CD8::GFP/+*. Green: Anti-GFP, Red: Anti-Akh, marking all CC cells, Blue: DAPI. Anti-GFP-channel only. b") Anti-Akh channel only

C-C") *w; StanEx^{DT-1}/+; LexAop-CD8::GFP/+*. Green: Anti-GFP, Red: Anti-Dilp2, marking all IPC cells, Blue: DAPI. a') Anti-GFP-channel only. c") Anti-Dilp2 channel only

Supplementary Figure and Table Legends

Suppl. Figure 1: Schematic map of molecular modules composing the StanEx P-element. The StanEx P-element is a derivative of the InSITE P-element (Grohl et al.,, NatMeth2011), expressing the LexA DNA-binding domain fused to the hinge and transcriptional activator domain of Gal4 (LexA::HG) under the control of the weak P-element promoter. P-element inverted repeats, loxP and phiC31 sites are present as indicated, enabling recombinase-mediated cassette exchange.

Suppl. Figure 2: Hybrid dysgenesis crossing scheme. The StanEx collection was generated by crossing the X-linked StanEx1 insertion to *Δ2-3* transposase, followed by the extraction of transposition events by crossing F_1 *w, StanEx*^{1} */ Y; Δ2-3, Sb* / + males to *w; CyO / L; TM6B, Tb, Hu / ftz, e* and selecting w^+ male offspring. Subsequently, the novel lines were balanced as indicated.

Suppl. Figure 3: Clustering of tissue specific expression data across StanEx lines. Euclidian distance was used. Red=Expression detected. Black=no expression detected or not examined.

Suppl. Figure 4: Immuno-histochemical analysis of patterned StanEx enhancer trap expression in third instar larval proventriculus visualized by *lexAop-CD8::GFP*. Green: Anti-GFP, Red: Anti-Tubulin, Blue: DAPI. Scale bar 50 μm

A-A') *w; StanEx*$^{IP-5}$*/+; LexAop-CD8::GFP/+*.

B-B') *w; StanEx*$^{DRH-4}$ */+; LexAop-CD8::GFP/+*.

C-C') *w; StanEx*$^{HS-2}$*/ LexAop-CD8::GFP*.

D-D') *w; StanEx*$^{CS-4}$*/+; LexAop-CD8::GFP/+*.

E-E') *w; StanEx*$^{EH-7}$*/LexAop-CD8::GFP*.

F-F') *w; StanEx*$^{EM-10}$*/LexAop-CD8::GFP*.

G-G') *w; StanEx*$^{DL-4}$*/LexAop-CD8::GFP*.

Suppl. Figure 5: Expression pattern of StanEx^{1} enhancer trap in tissues of wandering third instar larvae visualized by lexAop-CD8:GFP. Only the GFP channel is shown in green, corresponding to Figure 1. Green: Anti-GFP. Scale bar = 100 um.

A) CC cells in ring gland .
B) Expression in imaginal disc of wing, leg and haltere.
C) Eye disc.

D) Midgut. Note that expression in garland nephrocytes is lexAop-CD8::GFP background signal (see Methods and Suppl. Figure 6).

E) Fat body.

Suppl. Figure 6: Detection of GFP signal in *lexAop2-CD8::GFP* independently of LexA driver. A) Pericardial nephrocytes. B) Garland nephrocytes. Genotype: *yw; lexAop2-CD8::GFP / +*. Green: Anti-GFP, Blue: DAPI. Scalebar: 50um.

Suppl Table 1: Summary table of molecular data and expression characterization of the StanEx enhancer trap collection. The same information in a searchable format is available at the StanEx online database http://stanex.stanford.edu/about/. We defined the molecular coordinate of a P-element insertion into the genome as the first nucleotide 3' of the site where the P-element inserted, independently of the orientation of insertion.

Suppl. Table 2: Summary of StanEx enhancer trap lines analyzed for adult IPC and CC cell expression.

Acknowledgments

We thank Dr. Jordon Wang at Lakeview Pharma, and members of the Kim lab, especially Dr. R.W. Alfa, for helpful discussions. We thank Mr. T. Hassan, T. Hutton, Bill and Kathy MacAlpine, Richard Hook, Drs. J. Hessel, J. Blackwood, faculty colleagues at Exeter and Dr. W. Talbot at Stanford for advice, support and encouragement. S.K.K. dedicates this study to Kenneth G. Hook, Alice Hook and Dr. Richard Parris. Work in the Kim group was supported by the Howard Hughes Medical Institute (HHMI), the John and Eileen Hessel Fund for Innovation in Science Education at Phillips Exeter Academy, the H.L. Snyder Foundation, and the Elser Trust.

References

Alfa RW, Park S, Skelly KR, Poffenberger G, Jain N, Gu X, Kockel L, Wang J, Liu Y, Powers AC, Kim SK (2015). Suppression of insulin production and secretion by a decretin hormone. Cell Metab 21(2):323-33.

Ballinger DG, Benzer S (1989). Targeted gene mutations in *Drosophila*. Proc Natl Acad Sci U S A 86(23):9402-6.

Bateman JR, Johnson JE, Locke MN (2012). Comparing enhancer action in cis and in trans. Genetics 191(4):1143-55.

Bellen HJ, Levis RW, Liao G, He Y, Carlson JW, Tsang G, Evans-Holm M, Hiesinger PR, Schulze KL, Rubin GM, Hoskins RA, Spradling AC (2004). The BDGP gene disruption project: single transposon insertions associated with 40% of *Drosophila* genes. Genetics 167(2):761-81.

Bellen HJ, Levis RW, He Y, Carlson JW, Evans-Holm M, Bae E, Kim J, Metaxakis A, Savakis C, Schulze KL, Hoskins RA, Spradling AC (2011). The *Drosophila* gene disruption project: progress using transposons with distinctive site specificities. Genetics 188(3):731-43

Berg CA, Spradling AC (1991). Studies on the rate and site-specificity of P element transposition. Genetics 127(3):515-24.

Bosch JA, Tran NH, Hariharan IK (2015). CoinFLP: a system for efficient mosaic screening and for visualizing clonal boundaries in *Drosophila*. Development. 2015 Feb 1;142(3):597-606.

Brand AH, Perrimon N (1993). Targeted gene expression as a means of altering cell fates and generating dominant phenotypes. Development 118(2):401-15.

Call GB, et al., (2007). Genomewide clonal analysis of lethal mutations in the *Drosophila* melanogaster eye: comparison of the X chromosome and autosomes. Genetics 177:689-97.

Cognigni P, Bailey AP, Miguel-Aliaga I (2011). Enteric neurons and systemic signals couple nutritional and reproductive status with intestinal homeostasis. Cell Metab 13(1):92-104.

De Paola V, Holtmaat A, Knott G, Song S, Wilbrecht L, Caroni P, Svoboda K (2006). Cell type-specific structural plasticity of axonal branches and boutons in the adult neocortex. Neuron 49(6):861-75.

Gnerer JP, Venken KJ, Dierick HA (2015). Gene-specific cell labeling using MiMIC transposons. Nucleic Acids Res. 2015 Apr 30;43(8):e56.

Gohl DM, Silies MA, Gao XJ, Bhalerao S, Luongo FJ, Lin CC, Potter CJ, Clandinin TR (2011). A versatile in vivo system for directed dissection of gene expression patterns. Nat Methods 8(3):231-7.

Gordon MD, Scott K (2009). Motor control in a *Drosophila* taste circuit. Neuron 61(3):373-84.

Graveley BR, Brooks AN, Carlson JW, Duff MO, Landolin JM, Yang L, Artieri CG, van Baren MJ, Boley N, Booth BW, Brown JB, Cherbas L, Davis CA, Dobin A, Li R, Lin W, Malone JH, Mattiuzzo NR, Miller D, Sturgill D, Tuch BB, Zaleski C, Zhang D, Blanchette M, Dudoit S, Eads B, Green RE, Hammonds A, Jiang L, Kapranov P, Langton L, Perrimon N, Sandler JE, Wan KH, Willingham A, Zhang Y, Zou Y, Andrews J, Bickel PJ, Brenner SE, Brent MR, Cherbas P, Gingeras TR, Hoskins RA, Kaufman TC, Oliver B, Celniker SE (2011). The developmental transcriptome of *Drosophila* melanogaster. Nature 471(7339):473-9.

Groth AC, Fish M, Nusse R, Calos MP (2004). Construction of transgenic *Drosophila* by using the site-specific integrase from phage phiC31. Genetics 166(4):1775-82.

Han C, Jan LY, Jan YN (2011). Enhancer-driven membrane markers for analysis of nonautonomous mechanisms reveal neuron-glia interactions in *Drosophila*. Proc Natl Acad Sci U S A 108(23):9673-8.

Harvie PD, Filippova M, Bryant PJ (1998). Genes expressed in the ring gland, the major endocrine organ of *Drosophila* melanogaster. Genetics 149(1):217-31.

Hatfull GF, et al., (2006). Exploring the mycobacteriophage metaproteome: phage genomics as an educational platform. PLoS Genet 2:e92. Epub 2006 Jun 9.

Hayashi S, Ito K, Sado Y, Taniguchi M, Akimoto A, Takeuchi H, Aigaki T, Matsuzaki F, Nakagoshi H, Tanimura T, Ueda R, Uemura T, Yoshihara M, Goto S (2002). GETDB, a database compiling expression patterns and molecular locations of a collection of Gal4 enhancer traps. Genesis 34(1-2):58-61.

Hwang HJ, Rulifson E (2011). Serial specification of diverse neuroblast identities from a neurogenic placode by Notch and Egfr signaling. Development 138(14):2883-93.

Jenett A, Rubin GM, Ngo TT, Shepherd D, Murphy C, Dionne H, Pfeiffer BD, Cavallaro A, Hall D, Jeter J, Iyer N, Fetter D, Hausenfluck JH, Peng H, Trautman ET, Svirskas RR, Myers EW, Iwinski ZR, Aso Y, DePasquale GM, Enos A, Hulamm P, Lam SC, Li HH, Laverty TR, Long F, Qu L, Murphy SD, Rokicki K, Safford T, Shaw K, Simpson JH, Sowell A, Tae S, Yu Y, Zugates CT (2012). A GAL4-driver line resource for *Drosophila* neurobiology. Cell Rep 2(4):991-1001.

Josten F, Fuss B, Feix M, Meissner T, Hoch M (2004). Cooperation of JAK/STAT and Notch signaling in the *Drosophila* foregut. Dev Biol. 267(1):181-9.

Kassis JA (2012). Transvection in 2012: site-specific transgenes reveal a plethora of trans-regulatory effects. Genetics 2012 191(4):1037-9.

Kim SK, Rulifson EJ (2004). Conserved mechanisms of glucose sensing and regulation by *Drosophila* corpora cardiaca cells. Nature 431(7006):316-20.

Kim J, Neufeld TP (2015). Dietary sugar promotes systemic TOR activation in *Drosophila* through AKH-dependent selective secretion of Dilp3. Nat Commun 6:6846.

Kölzer S, Fuss B, Hoch M, Klein T (2003). Defective proventriculus is required for pattern formation along the proximodistal axis, cell proliferation and formation of veins in the *Drosophila* wing. Development 130(17):4135-47.

Korzelius J, Naumann SK, Loza-Coll MA, Chan JS, Dutta D, Oberheim J, Gläßer C, Southall TD, Brand AH, Jones DL, Edgar BA. (2014) Escargot maintains stemness and suppresses differentiation in Drosophila intestinal stem cells. EMBO J. 17;33(24):2967-82

Knapp JM, Chung P, Simpson JH (2015). Generating customized transgene landing sites and multi-transgene arrays in *Drosophila* using phiC31 integrase. Genetics 199(4):919-34.

Kroos L, Kaiser D (1984). Construction of Tn5 *lac*, a transposon that fuses *lacZ* expression to exogenous promoters, and its introduction into *Myxococcus xanthus*. *Proc Natl Acad Sci* USA 81, 5816-5820.

Lai SL, Lee T. (2006). Genetic mosaic with dual binary transcriptional systems in *Drosophila*. Nat Neurosci 9:703–709.

Li HH, Kroll JR, Lennox SM, Ogundeyi O, Jeter J, Depasquale G, Truman JW (2014). A GAL4 driver resource for developmental and behavioral studies on the larval CNS of *Drosophila*. Cell Rep 8(3):897-908.

Liao GC, Rehm EJ, Rubin GM (2000). Insertion site preferences of the P transposable element in *Drosophila* melanogaster. Proc Natl Acad Sci U S A 97(7):3347-51.

Macpherson LJ, Zaharieva EE, Kearney PJ, Alpert MH, Lin TY, Turan Z, Lee CH, Gallio M. (2015). Dynamic labelling of neural connections in multiple colours by trans-synaptic fluorescence complementation. Nat Commun. 6:10024.

Mellert DJ, Truman JW (2012). Transvection is common throughout the *Drosophila* genome. Genetics 191(4):1129-41.

Ochman H, Gerber AS, Hartl DL (1988). Genetic applications of an inverse polymerase chain reaction. Genetics 120: 621–623.

O'Hare K, Rubin GM (1983). Structures of P transposable elements and their sites of insertion and excision in the *Drosophila* melanogaster genome. Cell 34(1):25-35.

O'Kane CJ, Gehring WJ (1987). Detection in situ of genomic regulatory elements in *Drosophila*. Proc Natl Acad Sci U S A 84(24):9123-7.

Pankratz MJ, Hoch M (1995). Control of epithelial morphogenesis by cell signaling and integrin molecules in the *Drosophila* foregut. Development 121(6):1885-98.

Park S, Bustamante EL, Antonova J, McLean GW, Kim SK (2011). Specification of *Drosophila* corpora cardiaca neuroendocrine cells from mesoderm is regulated by Notch signaling. PLoS Genet. 7(8):e1002241.

Pfeiffer BD, Jenett A, Hammonds AS, Ngo TT, Misra S, Murphy C, Scully A, Carlson JW, Wan KH, Laverty TR, Mungall C, Svirskas R, Kadonaga JT, Doe CQ, Eisen MB, Celniker SE, Rubin GM (2008). Tools for neuroanatomy and neurogenetics in *Drosophila*. Proc Natl Acad Sci USA 105(28):9715-20.

Pfeiffer BD, Ngo TT, Hibbard KL, Murphy C, Jenett A, Truman JW, Rubin GM (2010). Refinement of tools for targeted gene expression in *Drosophila*. Genetics. 186(2):735-55.

Rajan A, Perrimon N (2011). *Drosophila* as a model for interorgan communication: lessons from studies on energy homeostasis. Dev Cell 21(1):29-31.

Rajan A, Perrimon N (2012). *Drosophila* cytokine unpaired 2 regulates physiological homeostasis by remotely controlling insulin secretion. Cell 151(1):123-37.

Redfield RJ (2012). "Why do we have to learn this stuff?"-A new genetics for 21st century students. PLoS Biol. 10(7):e1001356.

Ryder E, Blows F, Ashburner M, Bautista-Llacer R, Coulson D, Drummond J, Webster J, Gubb D, Gunton N, Johnson G, O'Kane CJ, Huen D, Sharma P, Asztalos Z, Baisch H, Schulze J, Kube M, Kittlaus K, Reuter G, Maroy P, Szidonya J, Rasmuson-Lestander A, Ekström K, Dickson B, Hugentobler C, Stocker H, Hafen E, Lepesant JA, Pflugfelder G, Heisenberg M, Mechler B, Serras F, Corominas M, Schneuwly S, Preat T, Roote J, Russell S (2004). The DrosDel collection: a set of P-element insertions for generating custom chromosomal aberrations in *Drosophila* melanogaster. Genetics 167(2):797-813.

Senger K, Armstrong GW, Rowell WJ, Kwan JM, Markstein M, Levine M (2004). Immunity regulatory DNAs share common organizational features in *Drosophila*. Mol Cell 13(1):19-32.

Senger K, Harris K, Levine M (2006). GATA factors participate in tissue-specific immune responses in *Drosophila* larvae. Proc Natl Acad Sci U S A 103(43):15957-62.

Sentry JW, Kaiser K (1994). Application of inverse PCR to site-selected mutagenesis of *Drosophila*. Nucleic Acids Research 22: 3429–3430.

Shim J, Mukherjee T, Mondal BC, Liu T, Young GC, Wijewarnasuriya DP, Banerjee U (2013). Olfactory control of blood progenitor maintenance. Cell 155(5):1141-53.

Singh SR, Zeng X, Zheng Z, Hou SX (2011). The adult *Drosophila* gastric and stomach organs are maintained by a multipotent stem cell pool at the foregut/midgut junction in the cardia (proventriculus). Cell Cycle 10(7):1109-20.

Spradling AC, Stern DM, Kiss I, Roote J, Laverty T, Rubin GM (1995). Gene disruptions using P transposable elements: an integral component of the *Drosophila* genome project. Proc Natl Acad Sci U S A 92(24):10824-30.

Szüts D, Bienz M (2000). LexA chimeras reveal the function of *Drosophila* Fos as a context-dependent transcriptional activator. Proc Natl Acad Sci U S A 97(10):5351-6.

Takashima S, Adams KL, Ortiz PA, Ying CT, Moridzadeh R, Younossi-Hartenstein A, Hartenstein V. (2011). Development of the Drosophila entero-endocrine lineage and its specification by the Notch signaling pathway. Dev Biol. 353(2):161-72.

Yagi R, Mayer F, Basler K (2010). Refined LexA transactivators and their use in combination with the *Drosophila* Gal4 system. Proc Natl Acad Sci U S A. 107(37):16166-71.

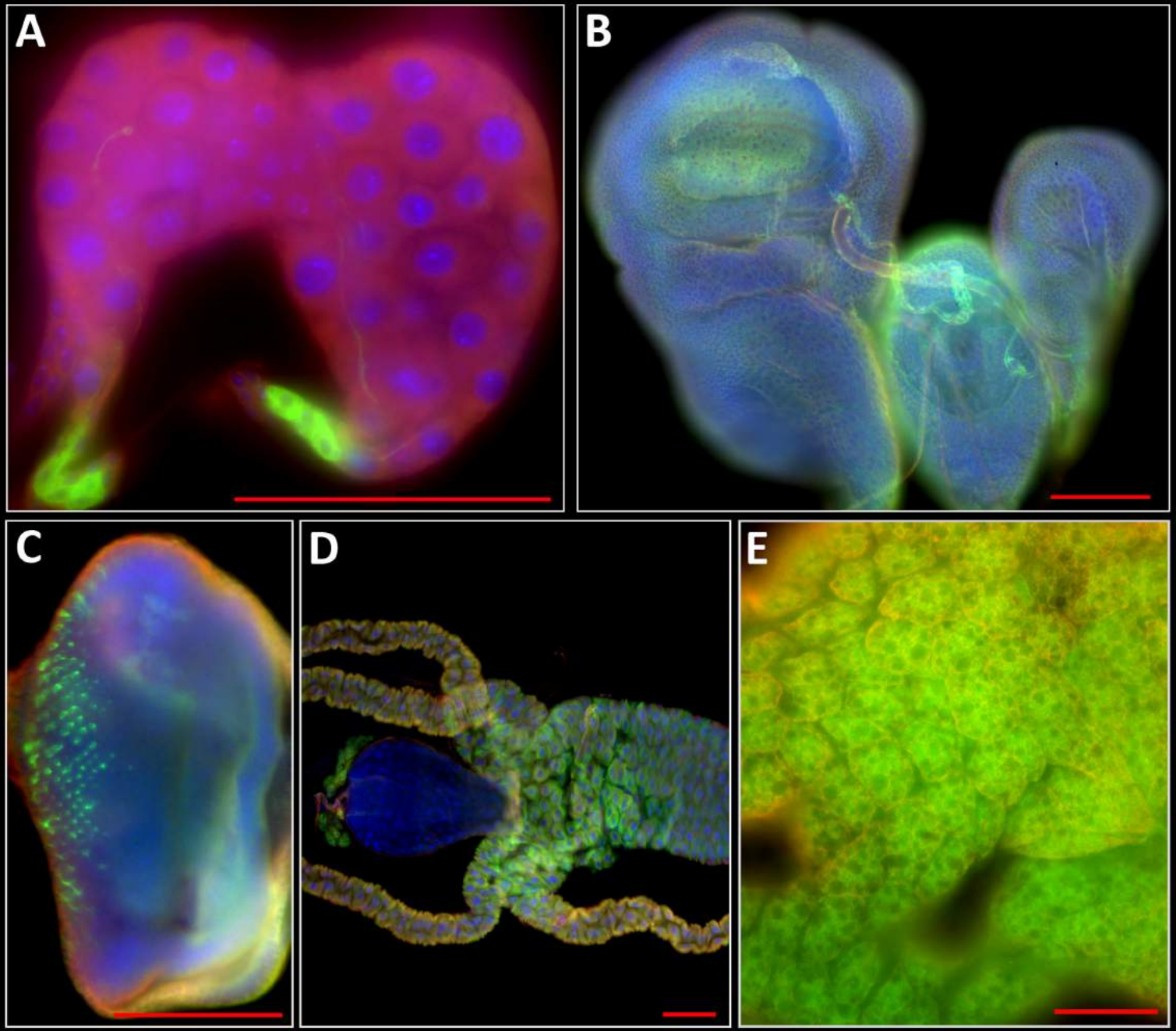
A
B
C
D
E

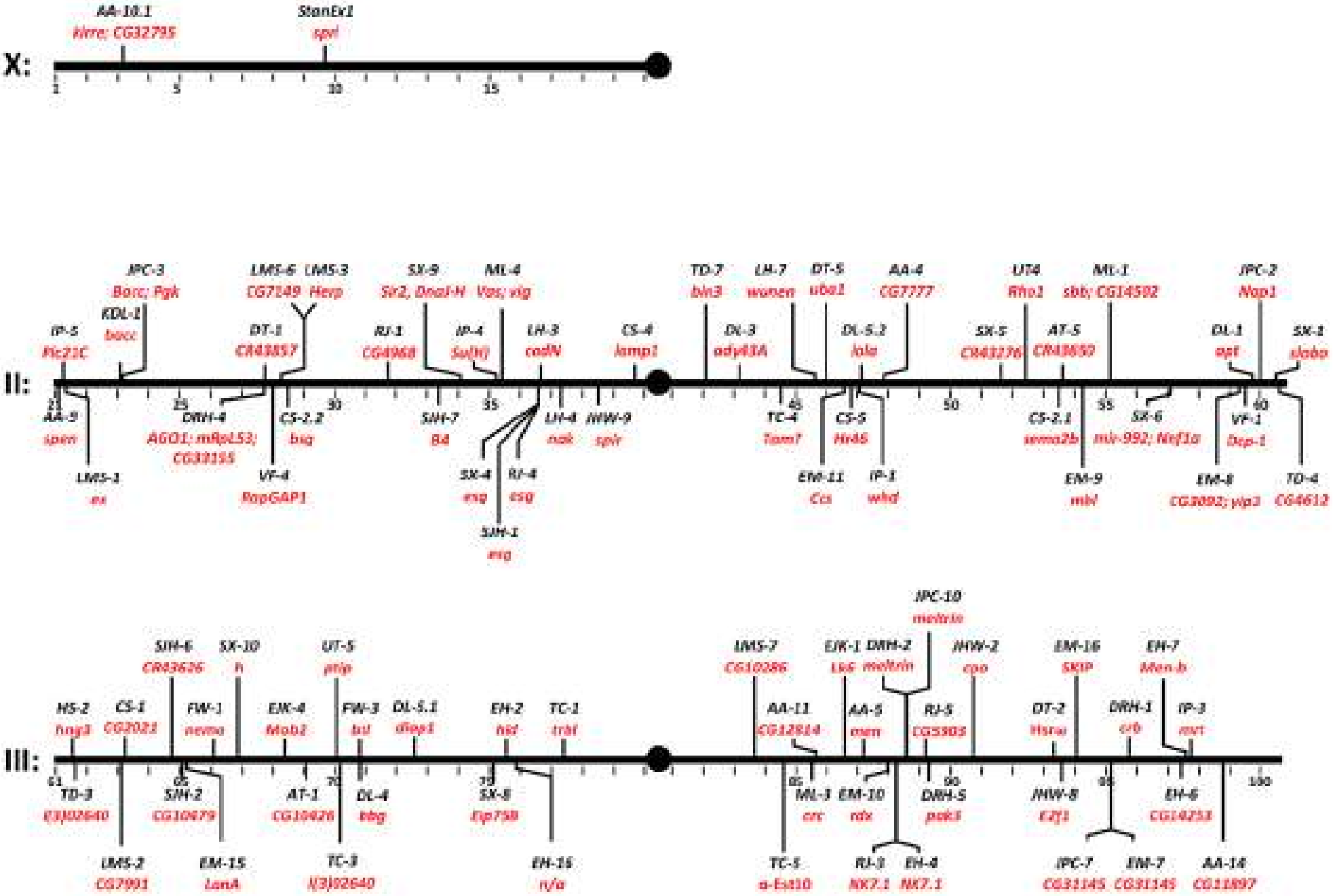
X:
AA-10.1
Nmre; CG32795
StanEx1
spri
1
5
10
15
II:
IP-5
Nic21C
KDL-1
bacc
JPC-3
Barc; Pgk
DT-1
CR43857
LMS-6
CG7149
LMS-3
Herp
RJ-1
CG4968
SX-9
Sir2; DnaJ-H
IP-4
Su(fu)
ML-4
Vas; vig
LH-3
codN
CS-4
lamp1
TD-7
bin3
DL-3
ody-6A
LH-7
wunen
DT-5
uba1
DL-5.2
lola
AA-4
CG7777
SX-5
CR43276
UT4
Rho1
AT-5
CR43850
ME-1
sbb; CG14592
DL-1
apt
JPC-2
Nap1
SX-1
slaba
AA-9
spen
DMH-4
AGO1; mRpL53; CG33155
CS-2.2
big
SJH-7
B4
LH-4
nak
JHW-9
spir
TC-4
Tom1
CS-5
Hr45
CS-2.1
sema2b
mir-992; Nelf1a
SX-6
VP-1
Dcp-1
LMS-1
ex
VP-4
RapGAP1
SX-4
exg
RJ-4
esg
SJH-1
mg
EM-11
Cct
IP-1
whd
EM-9
mbl
EM-8
CG3892; vip3
TD-4
CG4612
III:
HS-2
hng3
CS-1
CG32021
SJH-6
CR43626
FW-1
nemo
SX-10
h
EMK-4
Mob2
UT-5
ptip
FW-3
lzd
DL-5.1
dlgp1
EH-2
Nbf
TC-1
trbl
IMS-7
CG10286
AA-11
CG12814
EJK-1
Lbc
DMH-2
meltrin
IPC-10
meltrin
JHW-2
cpo
AA-5
mam
RJ-5
CG5385
EM-16
SKIP
DT-2
Hsrw
EH-7
Men-b
DRH-1
r/b
IP-3
mrt
TD-3
l(3)02640
LMS-2
CG7991
SJH-2
CG10479
EM-15
LanA
AT-1
CG10926
DL-4
klg
TC-3
l(3)02640
SX-8
Elp75B
EH-15
n/a
ML-3
crc
TC-5
a-Est10
EM-10
rdx
RJ-3
NK7.1
EH-4
NK7.1
DMH-5
poks1
JHW-8
EZ1
IPC-7
CG31145
EM-7
CG31145
EH-6
CG14253
AA-14
CG11897
61
65
70
75
80
85
90
95
100

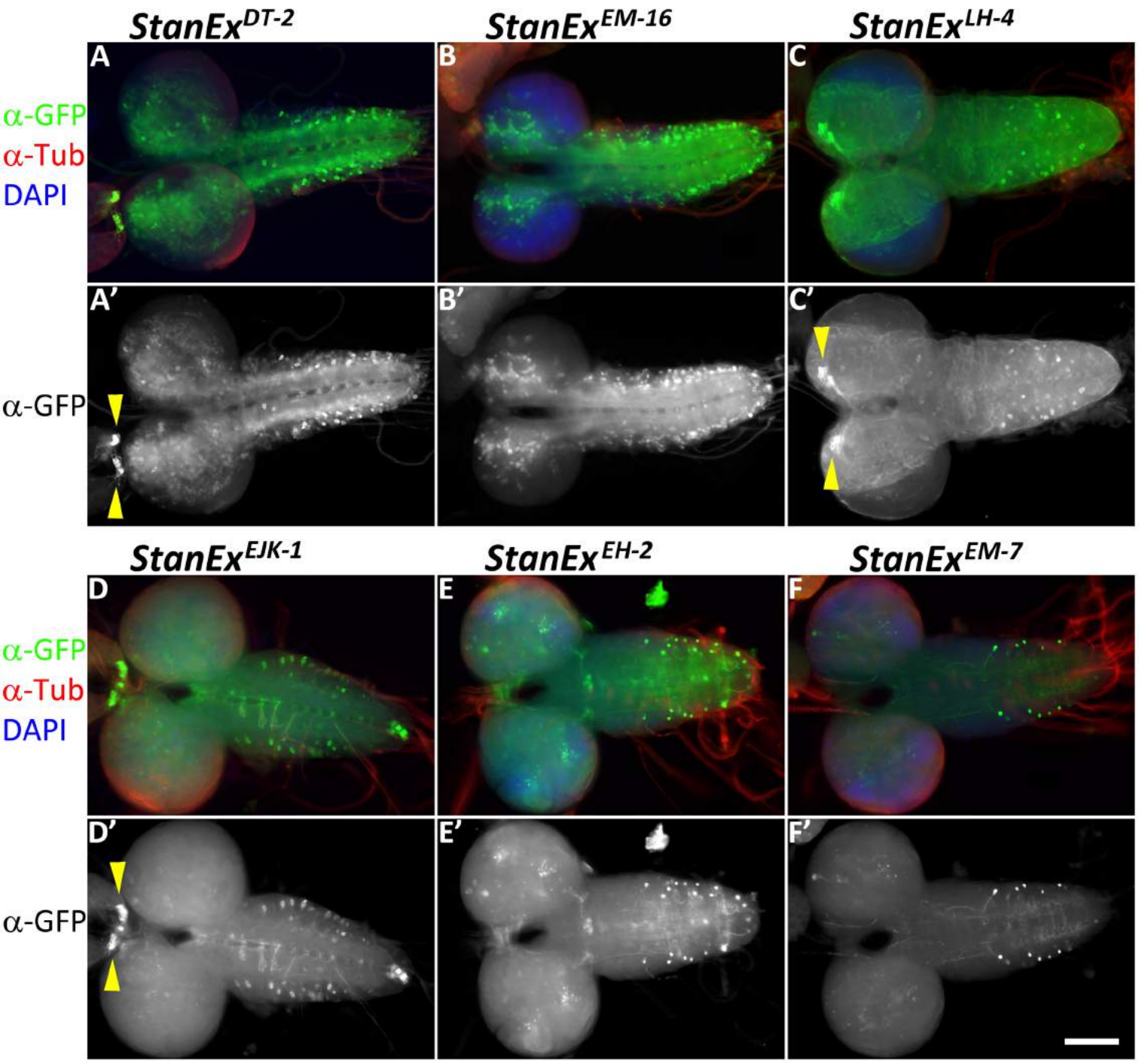
StanEx^DT-2
StanEx^EM-16
StanEx^LH-4
A
B
C
α-GFP
α-Tub
DAPI
A'
B'
C'
α-GFP
StanEx^EJK-1
StanEx^EH-2
StanEx^EM-7
D
E
F
α-GFP
α-Tub
DAPI
D'
E'
F'
α-GFP

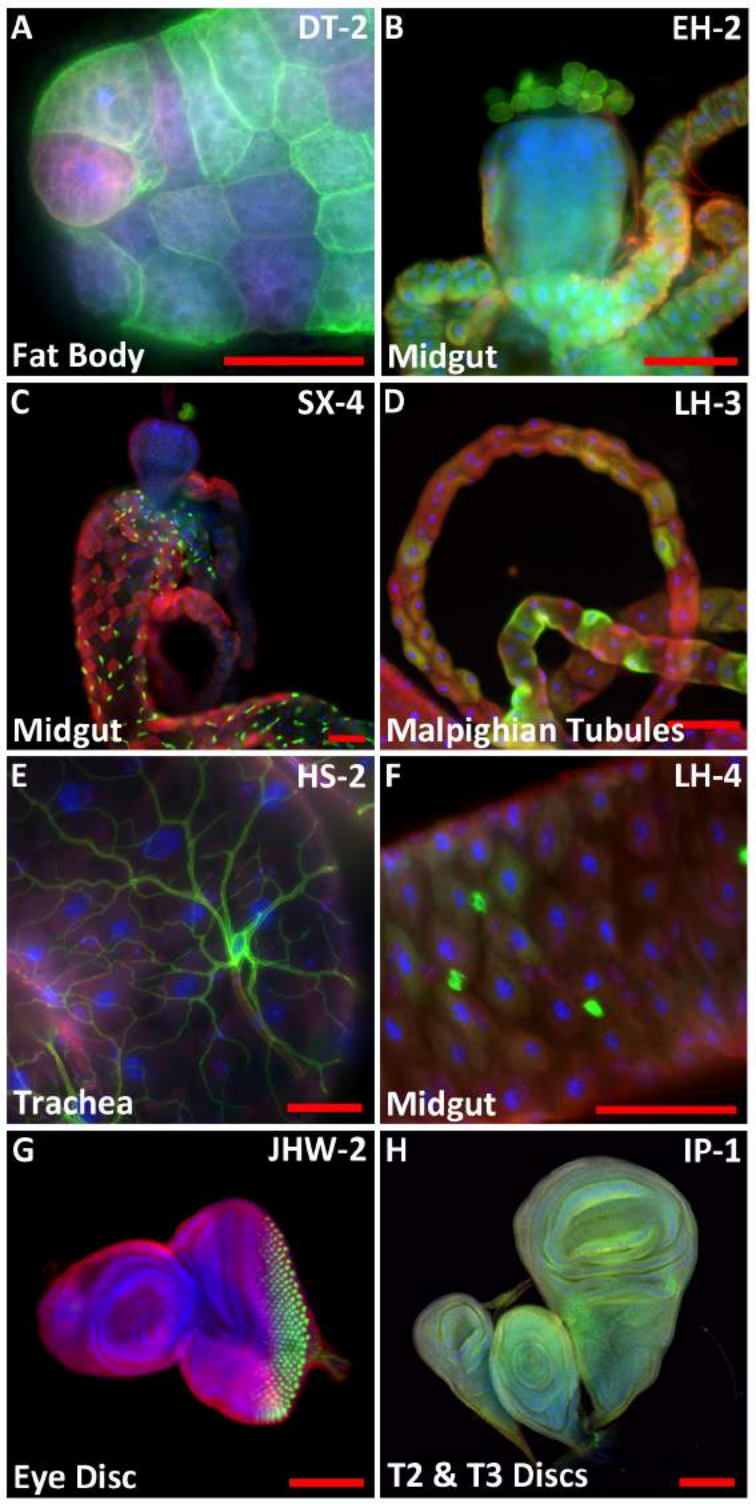
A
DT-2
Fat Body
B
EH-2
Midgut
C
SX-4
Midgut
D
LH-3
Malpighian Tubules
E
HS-2
Trachea
F
LH-4
Midgut
G
JHW-2
Eye Disc
H
IP-1
T2 & T3 Discs

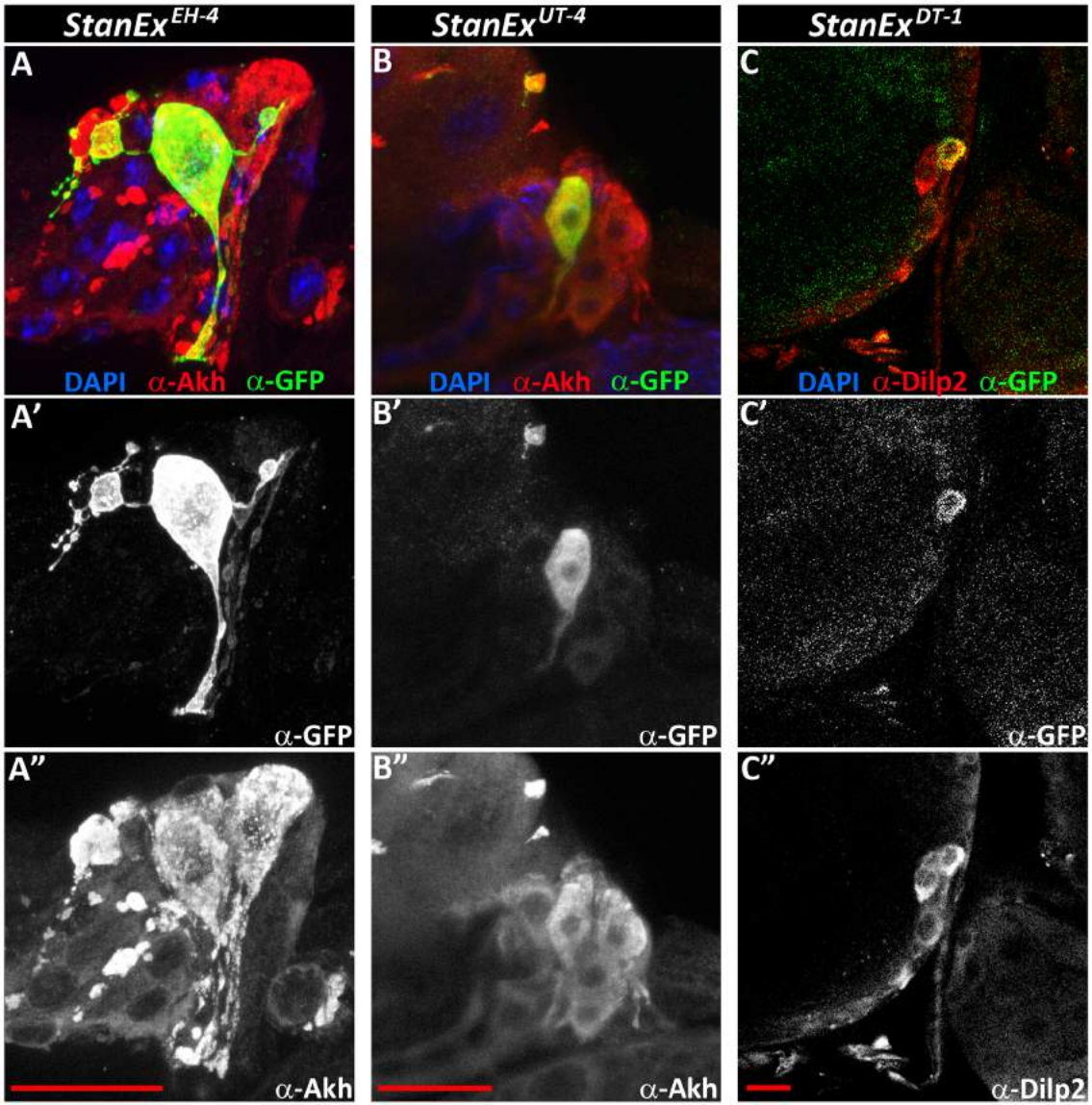
StanEx EH-4
StanEx UT-4
StanEx DT-1
A
B
C
DAPI α-Akh α-GFP
DAPI α-Akh α-GFP
DAPI α-Dilp2 α-GFP
A'
B'
C'
α-GFP
α-GFP
α-GFP
A"
B"
C"
α-Akh
α-Akh
α-Dilp2

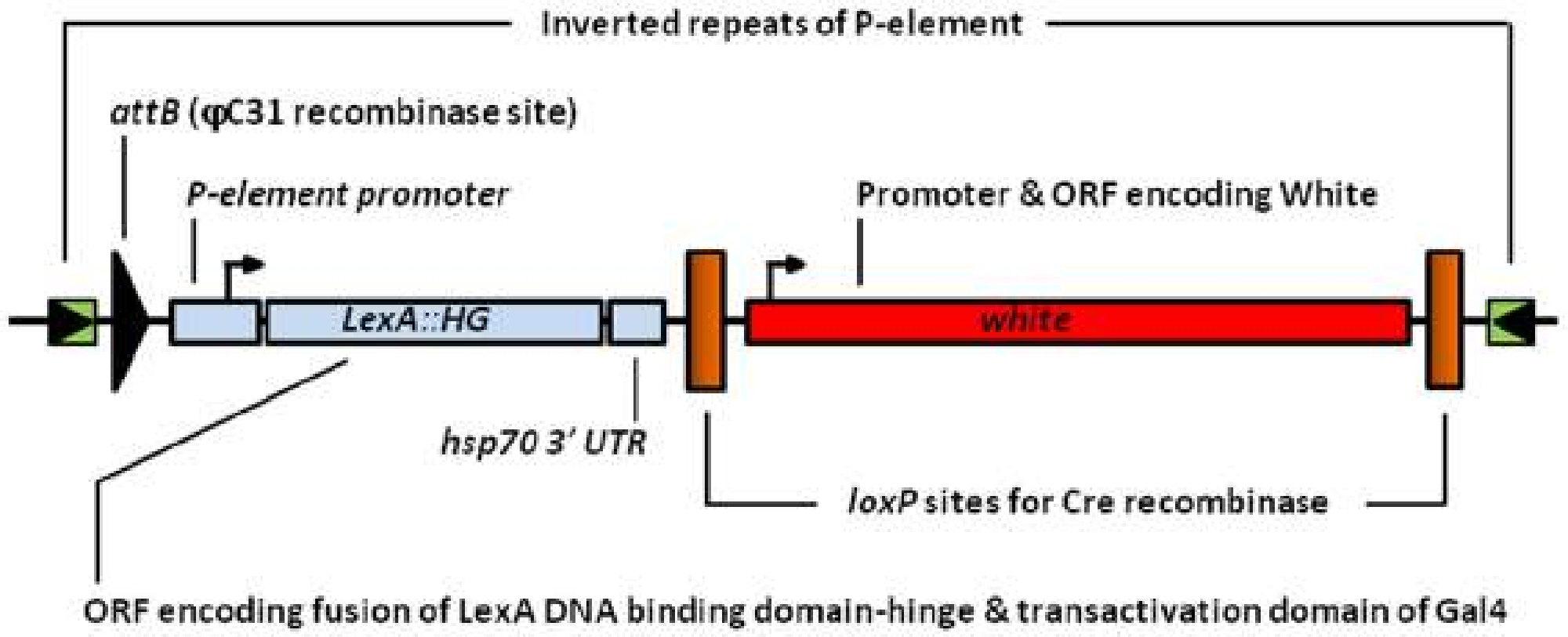
Inverted repeats of P-element
attB (φC31 recombinase site)
P-element promoter
Promoter & ORF encoding White
LexA::HG
white
hsp70 3' UTR
loxP sites for Cre recombinase
ORF encoding fusion of LexA DNA binding domain-hinge & transactivation domain of Gal4

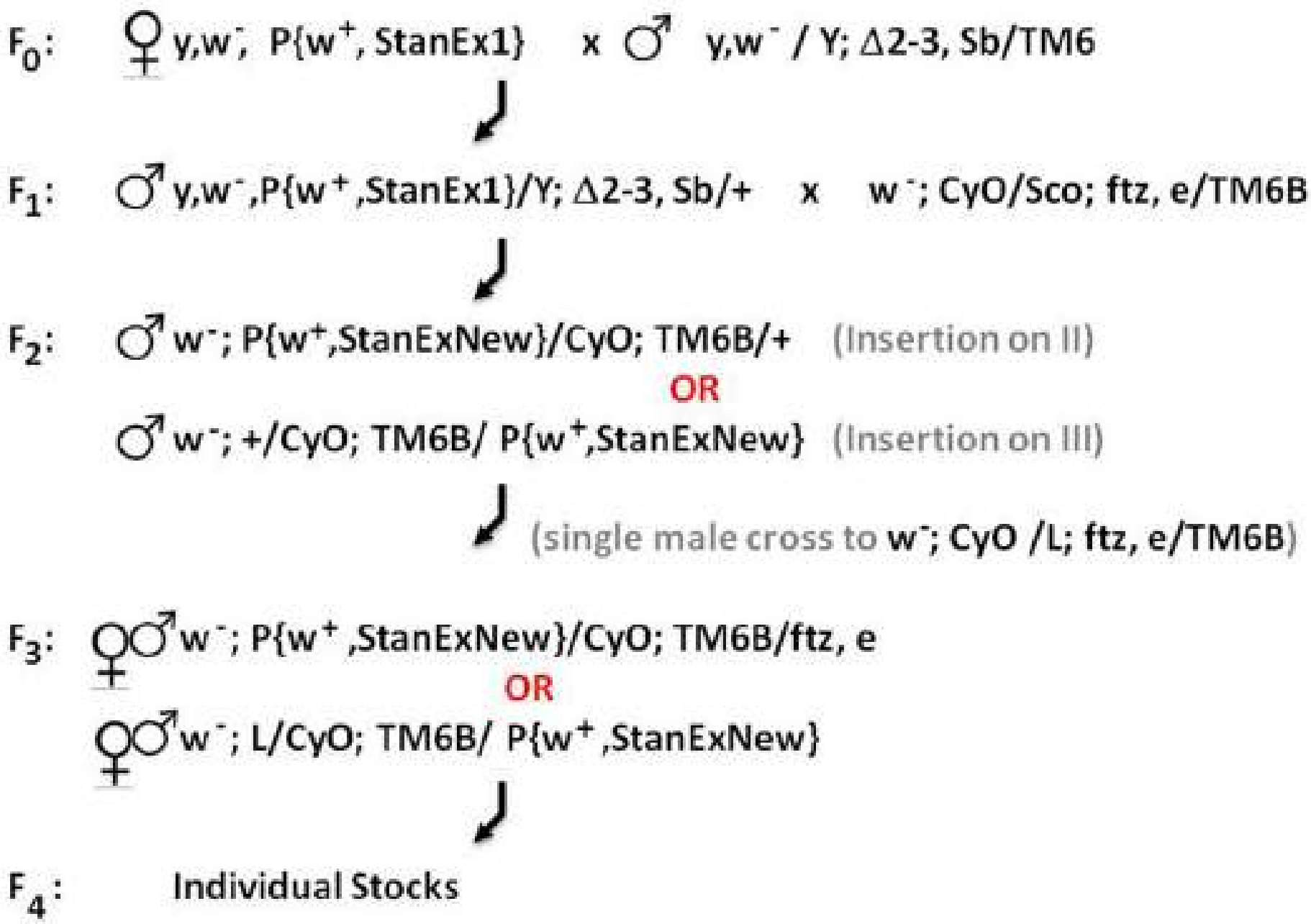
F0: ♀ y,w-, P{w+, StanEx1} x ♂ y,w- / Y; Δ2-3, Sb/TM6
F1: ♂ y,w-,P{w+,StanEx1}/Y; Δ2-3, Sb/+ x w-; CyO/Sco; ftz, e/TM6B
F2: ♂ w-; P{w+,StanExNew}/CyO; TM6B/+ (Insertion on II)
OR
♂ w-; +/CyO; TM6B/ P{w+,StanExNew} (Insertion on III)
(single male cross to w-; CyO /L; ftz, e/TM6B)
F3: ♀♂ w-; P{w+,StanExNew}/CyO; TM6B/ftz, e
OR
♀♂ w-; L/CyO; TM6B/ P{w+,StanExNew}
F4: Individual Stocks

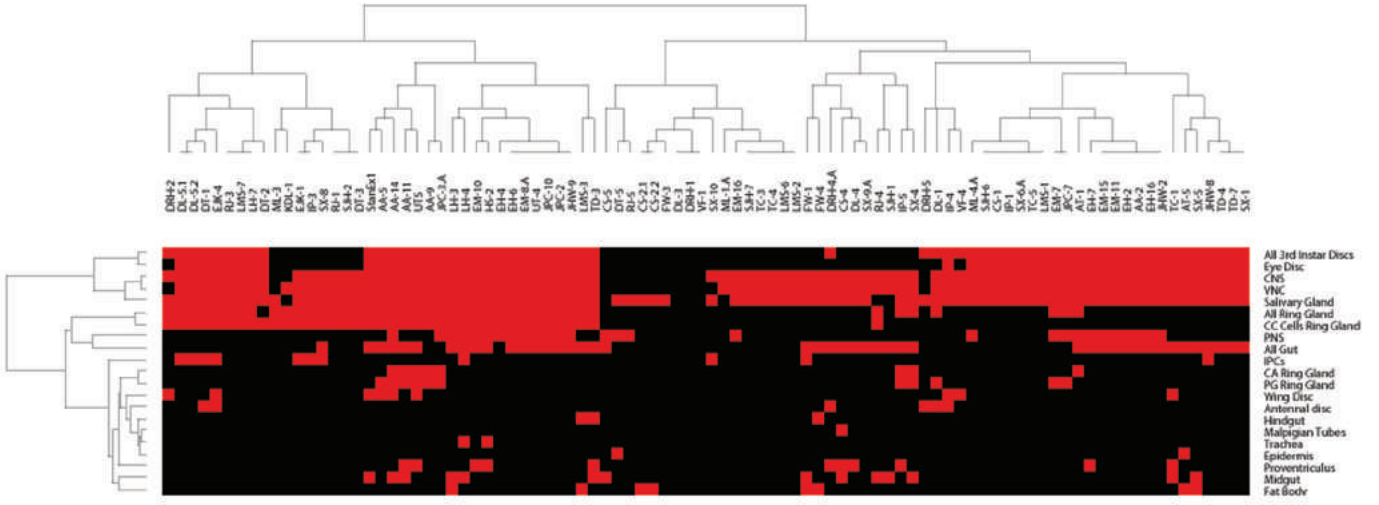
DB4-2
DC-3-1
DC-3-2
DT-1
EJK-4
RJ-3
LM5-7
LH-7
DL-2
ML-3
KDL-1
EJK-1
IP-3
SX-8
SH-1
SH-2
DT-3
Stan6X1
AA-5
AA-14
AA-11
LH-5
AH-9
JPC-3A
LH-3
LH-4
EM-10
HP-2
EH-4
EH-6
EM-8A
UT-4
JPC-10
JPC-7
JPC-9
LM5-3
TD-3
CS-5
DT-5
RJ-5
CS-23
FW-3
DL-3
DB4-1
VF-1
SE-10
ML-4A
EM-16
SH-7
TC-3
TC-4
LM5-6
LM5-2
FW-1
FW-4
DB4-4A
CS-4
DL-4
DL-6A
RJ-4
SH-1
IP-5
SX-4
DB4-5
IP-7
IP-4
VF-4
ML-4A
SH-6
CS-1
IP-1
SE-6A
TC-5
LM5-1
EM-7
JPC-7
AE-1
EH-1
EM-15
EM-11
EH-2
AA-2
EH-16
JHW-2
TC-1
AE-5
SX-5
JHW-8
TD-4
TD-7
SX-1
All 3rd Instar Discs
Eye Disc
CNS
VNC
Salivary Gland
All Ring Gland
CC Cells Ring Gland
PNS
All Gut
IPCs
CA Ring Gland
PG Ring Gland
Wing Disc
Antennal disc
Hindgut
Malpigian Tubes
Trachea
Epidermis
Proventriculus
Midgut
Fat Body

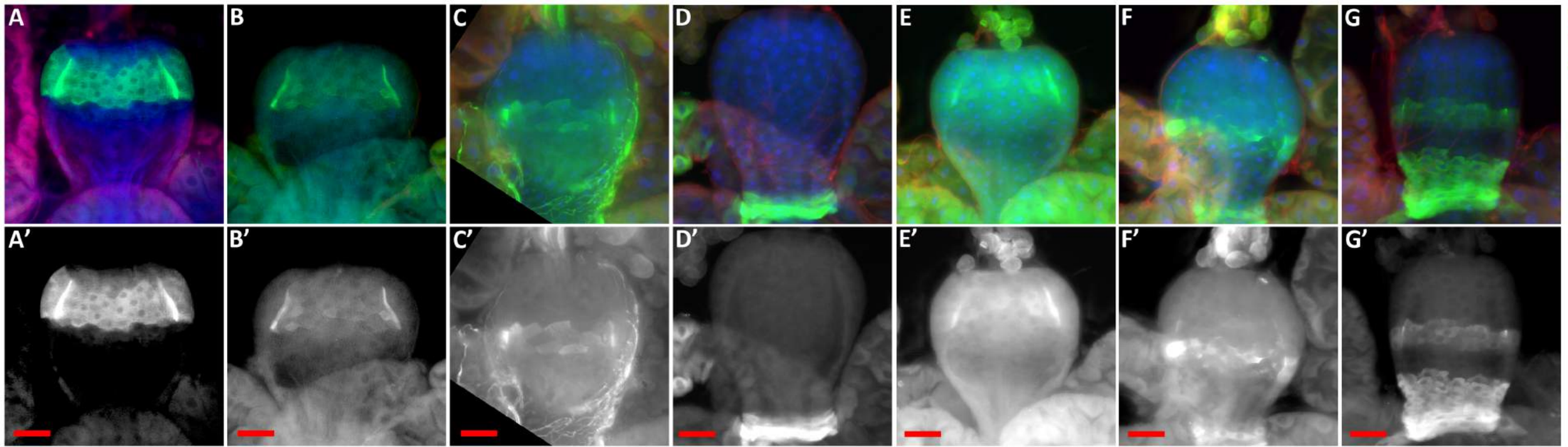
A
B
C
D
E
F
G
DAPI
Tubulin
GFP
A'
B'
C'
D'
E'
F'
G'
GFP
IP-5
DRH-4
HS-2
CS-4
EH-7
EM-10
DL-4

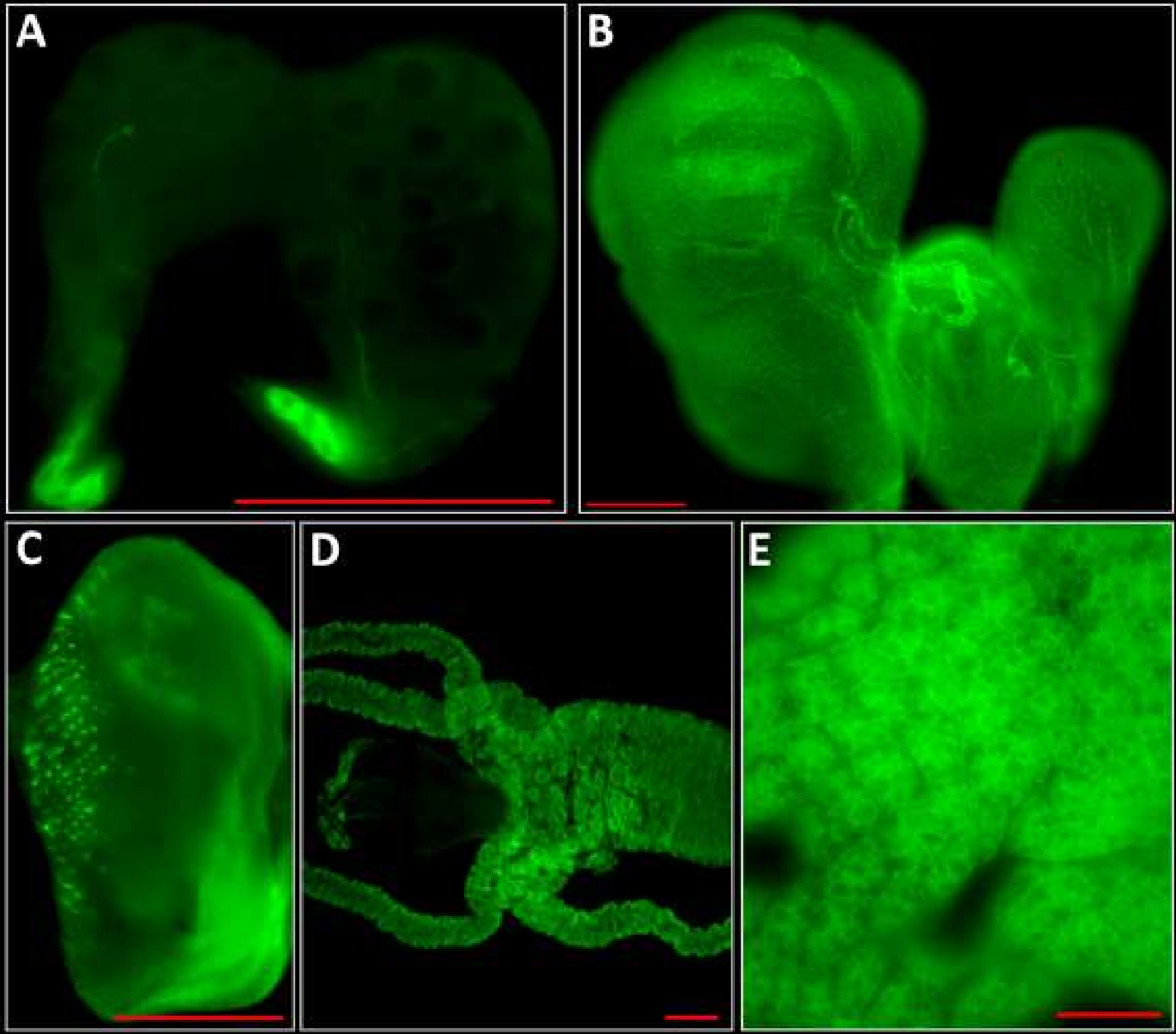
A
B
C
D
E

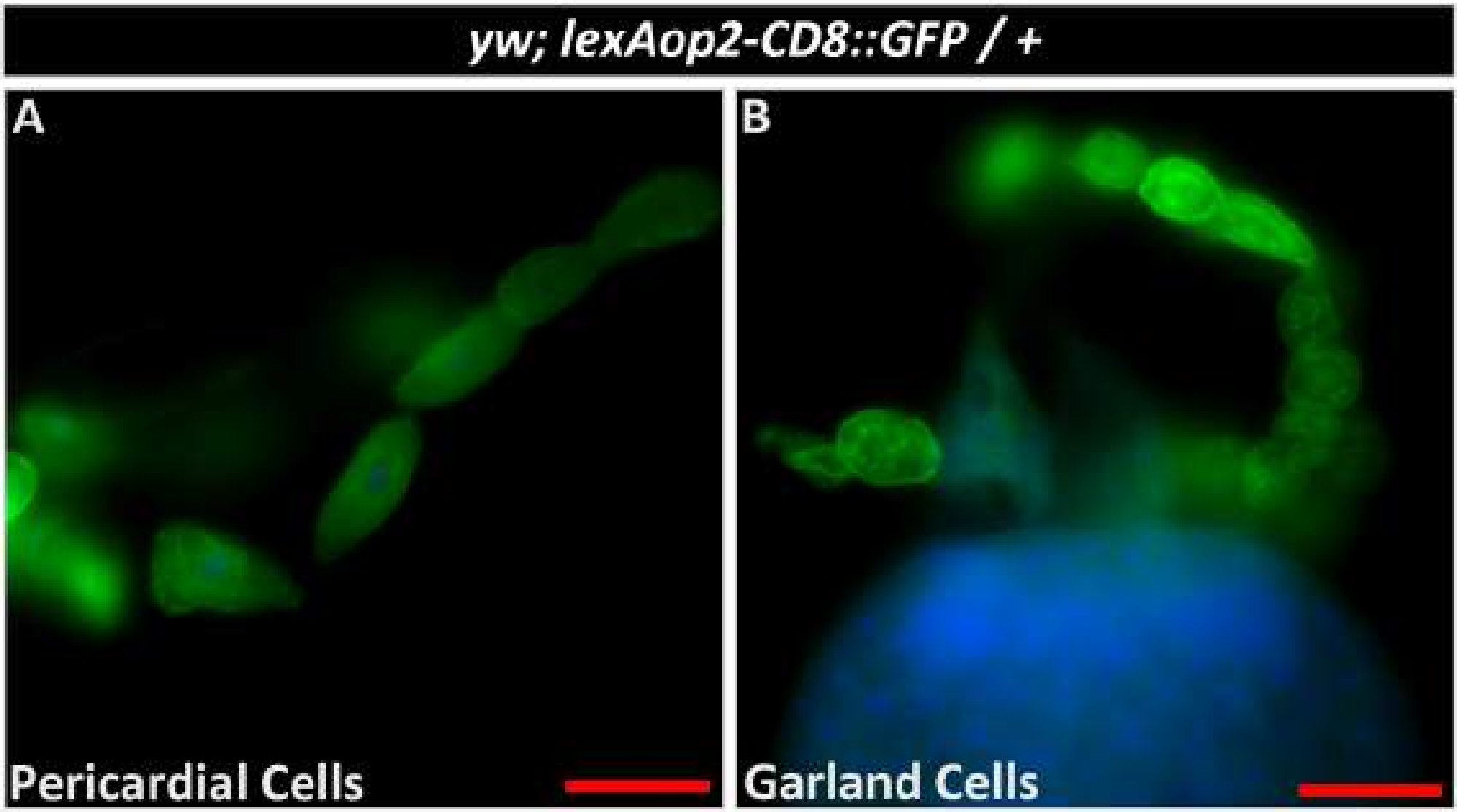
yw; lexAop2-CD8::GFP / +
A
Pericardial Cells
B
Garland Cells

Suppl. Table 2 Kockel et al. 2016

Line	IPC in Adult	CC Cells in Adult
SX-10	No	No
SX-8	No	Yes
SX-5	n/d	Yes
StanEx1	No	Yes
SJH-1	n/d	Yes
RJ-1	n/d	No
LMS-7	n/d	No
JHW-8	No	n/d
IP-4	n/d	Yes
EM-10	No	n/d
EM-8	n/d	Yes
EM-7	No	Yes
EH-4	n/d	Yes
DT-3	n/d	No
DT-1	n/d	No
DL-5	Yes	n/d
AT-5	n/d	No